Journal of CO2 Utilization 62 (2022) 102078

Contents lists available at ScienceDirect

Journal of CO2 Utilization

journal homepage: www.elsevier.com/locate/jcou

Investigation of steam and CO_2 gasification for biochar using a circulating fluidized bed gasifier model in Aspen HYSYS

Furkan Kartal, Senem Sezer, Uğur Özveren *

Department of Chemical Engineering, Marmara University, Goztepe Campus, Kadikoy, 34722 Istanbul, Turkey

ARTICLE INFO

Keywords:
CO_2 Gasification
Steam Gasification
Biochar
Fluidized Bed Gasifier
Aspen HYSYS

ABSTRACT

Researchers are focusing their efforts on renewable energy sources to avoid future global energy and environmental crises. One of the renewable energy sources, biomass, can be processed using a variety of techniques and thermodynamic cycles. Biomass gasification, for example, has several environmental and technical benefits. Biochar, on the other hand, is produced by the use of a thermal pretreatment technique to biomass, and it can be used to overcome the drawbacks of biomass in gasification operations. Despite the fact that biochar improves the quality and volume of syngas, there is a few research on this topic in the literature.

Although researchers have used a variety of process simulators, the number of gasification systems developed in the Aspen HYSYS simulator is very limited, and no circulating fluidized bed (CFB) gasification model for biochar gasification has ever been reported to our knowledge. Based on the non-stoichiometric equilibrium technique, a unique CFB gasifier model was developed in this work. The impacts of various operating parameters on the syngas were evaluated. In addition, the gasification performance of 10 biochar samples with varying physicochemical features was compared to the physicochemical qualities of solid fuels in a steam and CO_2 mixture. As a result, biochar samples with a high carbon content formed an H_2-rich syngas with a high calorific value during steam gasification. According to parametric studies, the optimum gasification temperature is about 700 °C, the optimum gasification pressure is 1 bar, and the optimum ratios of steam/biochar and CO_2/biochar are between 0.2–0.3 and 0.5–1.0, respectively.

1. Introduction

With the increasing depletion of fossil fuels and the rising demand for electricity, effective power generation from renewable energy sources is more important than ever before [1]. Coal, oil, and natural gas, on the other hand, are all key energy sources in today's civilizations. Managing the energy crisis while also lowering greenhouse gas emissions is undoubtedly one of the world's most difficult challenges [2,3]. Hence, scientists have been encouraged to examine alternative energy sources such as biomass and other renewable energy sources as a result of rapid global warming and climate change caused by the fossil fuel consumption [4]. The fact that biomass is carbon-neutral has led to a widespread awareness of biomass as a significant alternative energy source. Any biomass can be employed as a possible source of energy for the hydrogen-producing process. Woody biomass, on the other hand, is a better choice for generating heat and electricity than other biomass sources due to its high energy intensity and relatively large fixed carbon content [5].

Only a few lignocellulosic biomass-based alternatives offer nutritional value for traditional applications like feeding, while the majority are discarded and exploited as crude energy sources [6]. As a consequence, their removal, dumping, and incineration lead to a variety of serious environmental and marine problems [7]. Syngas production from biomass is more appealing due to lower production costs and the elimination of long-term environmental damage. In terms of syngas production, gasification appears to be the most advantageous of the thermochemical energy conversion techniques since it yields more beneficial gas components than any other method [8]. Gasification is the thermochemical conversion of any carbonaceous material into a gaseous fuel via partial oxidation with gasifying agents such as air, steam, oxygen, or mixtures of these agents [9]. The producer gas can be employed as fuel in gas engines, furnaces, boilers, and gas turbines, or it can be used to synthesize high-value chemicals [10].

The gasification process is greatly influenced by the gasifier's configuration, the type of feedstock used, and the gasification agent used in the reaction. In general, commercial gasification reactors are

* Corresponding author.
E-mail address: ugur.ozveren@marmara.edu.tr (U. Özveren).

https://doi.org/10.1016/j.jcou.2022.102078
Received 12 April 2022; Received in revised form 13 May 2022; Accepted 1 June 2022
Available online 6 June 2022

categorized as entrained bed, fluidized bed, or fixed bed based on their configuration and method of heating. Fluidized bed gasifiers allow high reaction rates that enhance the volatile production phase [11]. Also, high reaction rates, high flue gas temperatures, and low tar content in the produced gas are all common features of fluidized bed gasifiers [12]. When compared to bubbling fluidized bed gasifiers, circulating fluidized bed (CFB) gasifiers provide several advantages since they achieve a good level of turbulence, improve volumetric capacity, and store heat more efficiently [13]. Additionally, steam is typically chosen over other gasification agents because it can produce high-quality syngas [14], and steam gasification produces mostly H_2, CO, and CH_4 [15]. CO_2 can also be employed as a gasifying agent; however, it is less commonly used. CO_2 reacts with carbon and creates almost completely CO, enhancing carbon conversion efficiency while also allowing for the utilization of CO_2-captured emissions from industry [16]. The major problem in CO_2 gasification is the endothermic nature of the Boudouard reaction, which transforms CO_2 into CO. The heat necessary for this reaction has been proposed in a variety of ways [17]. The H_2/CO ratio in produced syngas may be successfully manipulated by combining H_2O and CO_2 in gasifying agent combinations at particular compositions, depending on the desired end uses. Furthermore, the char gasification is getting popular as a unique concept since it produces more syngas than raw biomass gasification [18]. Since devolatilization removes a portion of the volatiles from biomass and resulting in the formation of biochar, less tar is produced during biochar gasification. Additionally, since biochar includes a higher concentration of fixed carbon than raw biomass, its calorific value is significantly higher [19]. In addition, devolatilization procedure improves the atomic C/H and C/O ratios while also increasing reactivity. Therefore, char's enhanced reactivity contributes to increased syngas production [20]. Nonetheless, it is undeniable that the biochar gasification research is limited [21].

Chemkin, Aspen Plus, Open Foams, Aspen HYSYS, and Fluent are examples of commercially accessible computer-based modeling and simulation tools; they offer to investigate the effect of operating parameters and providing a good description of both chemical and physical phenomena in the gasifier, allowing an assessment of the plant's behavior in order to optimize gasifier design and operation with the least amount of time and money [22]. Among all of these programs, Aspen Plus is the most extensively used for thermochemical process simulations, especially including solid-state materials. Many researchers have extensively used Aspen Plus software to investigate biomass gasification [23–25], coal gasification [26–28], and co-gasification [29,30] processes. Aspen Plus is appropriate for analyzing solids since it has a built-in library model for computing solid properties. Apart from that, since Aspen Plus is linked to Fortran, an imperative computer language for numerical calculation tasks, adjustments and numerical computations are possible [31]. For the synthesis of H_2-rich syngas, Faraji et al. [32] suggested an integrated model of pyrolysis and air gasification system of various algal biomass. Authors indicated that the ideal operating parameters for increasing H_2 and CO production are 600 °C temperature, 1 atm pressure, and 0.01 m^3/h flow rate as a result of their parametric tests to improve the gasifier performance. The authors also stated that the gasification process at high pressures promotes CO_2 and char formation. Gopaul et al. [33] used the ASPEN Plus simulator to compare the synthesis of hydrogen from two chemical looping gasification techniques. The parametric study included temperature and pressure assessments on the primary reactors, and the simulated biomass material was poultry litter. According to the researchers, the atmospheric pressure was appropriate in all scenarios since greater pressures enhanced the yields of tar, H_2O, and CO_2. In another air gasification simulation in Aspen Plus, Hoo et al. [34] gasified the Napier grass sample in a fluidized bed gasifier model. The impact of operational variables such as gasification temperature, pressure, equivalence ratio, and moisture content was investigated in their study. As pressure increased from 1 to 20 atm, the lower heating value of syngas reduced from 1.9486 MJ/Nm^3 to 1.9339 MJ/Nm^3. Vikram et al. [35] used Aspen Plus to conduct a thermodynamic assessment for steam-carbon dioxide gasification of wood residue sample. Their findings showed that increasing CO_2 inclusion in steam enhanced CO synthesis as a result of the Boudouard reaction, leading to decreased H_2/CO ratio. H_2/CO ratio, on the other hand, increased with the rise in carbon dioxide/biomass ratio since a significant reduction in CO volume is observed due to water gas shift reaction and dilution of product stream by excess CO_2. Moreover, in another comparative Aspen Plus simulation study conducted by Islam [36], the researcher discussed the effect of various gasification agents (air, steam, CO_2, oxygen, H_2O_2) on syngas characteristics. According to the author, in a steam environment, the H_2/CO molar ratio, hydrogen%, and hydrogen yield were the greatest, but under a CO_2 atmosphere, the methane%, carbon monoxide%, CO yield, and lower heating values were the highest. Given the benefits of both atmospheres to the gasification process, the steam/CO_2 atmosphere appears to be a suitable agent for achieving the desired syngas quality and composition.

On the other hand, only a few number of Aspen HYSYS fluidized bed gasifiers have been reported. For date palm waste gasification, Bassyouni et al. [37] used Aspen HYSYS to design a downdraft gasifier model. The authors developed a set of six reactor unit blocks to model distinct downdraft gasification reaction regions. Their verified model can accurately forecast syngas composition and be used to identify the most appropriate operating conditions. Also, Gonzalez et al. [38] investigated the gasification process in Aspen HYSYS to assess H_2 generation from crude oil refinery waste. The researchers found that the equivalent air and steam/oil sludge ratios were 0.25–0.37 and 0.2–1.5, respectively, when analyzing gasification parameters such as temperature, syngas composition, and gas yield. Milani et al. [39] set out to propose and investigate different alternatives for combining concentrated solar power with biomass for power generation via gasification. As a summary of their results, authors observed that the identical gasifier model might have varied cost and technical performance depending on which of the three proposed combined cycles was used. However, the authors recommend that future research consider the impact of the gasifier model on overall performance. More recent studies were published by Kartal et al. [40] and Pashchenko [41] using Aspen HYSYS simulator. Kartal et al. designed a bubbling bed gasifier model to study the gasification properties of agricultural and animal wastes, and Pashchenko performed a thermodynamic analysis of the gasification process to determine the effectiveness of using thermochemical waste-heat recuperation systems by coal gasification. According to Kartal et al., the optimal steam/biomass ratio is 0.2–0.3, and the optimal gasifier temperature is 700–800 °C for producing high-quality syngas. Despite the fact that the number of biochar gasification systems is limited, simulation studies on biochar gasification systems have recently been published. In terms of cold gas efficiency, hydrogen content in syngas product, gasification system efficiency, total net heat, and CO_2 emission ratio, Kraisornkachit et al. [42] studied and compared the performance of several integrated systems of biochar gasifier and reformer. The authors examined each integrated system using mangrove tree charcoal samples at varying operating temperatures and feed ratios. Using Aspen Plus software, they utilized H_2O, CO_2, and O_2 as gasification mediums. According to their findings, raising the reformer temperature can improve cold gas efficiency and reduce CO_2 emissions in combined gasifier and reformer systems. They also indicated that the best O_2/feed ratio and the best H_2O/feed ratio for the maximum cold gas efficiency is 0.2 and 1.2, respectively. Despite the fact that the authors investigated at several different biochar gasification systems and found substantial findings, they only evaluated one biochar sample. That is, there is no evidence that fuel properties have an impact on thermodynamic or environmental performance. The authors also profited from the widely used Aspen Plus software. As mentioned in the previous sections, Aspen Plus has a strong database for the solid process simulations. Moreover, Zhang et al. [43] investigated bio-methanol synthesis by gasification of pine biomass, biochar, and pyrolysis oil using the process modeling program Aspen Plus. The results of the sensitivity

analysis performed in the researchers' study were in a techno-economic context, and only one biochar was used, similar to the other researchers referenced. Recently, Salaudeen et al. [44] published a research that is similar to our study. Using the Aspen Plus process simulator, the authors conducted a numerical analysis of steam gasification of hydrochar obtained from fruit wastes. They examined how different operation parameters and hydrochar properties affected syngas composition and heating value. Furthermore, the effectiveness of steam gasification of coir pith and its char is evaluated by AlNouss et al. [21]. The authors used Aspen Plus software to run parametric simulations and evaluate the gasification performance of biomass and biochar. According to their findings, steam gasification of biochar can produce high-quality syngas, and biochar gasification is more cost-effective than biomass gasification. However, there were no findings on the effect of biochar characteristics on syngas properties; the study was more on the biomass and biochar comparison. A comparison of the current study's findings with those found in the literature is summarized in Table 1.

To summarize, modeling studies of the biochar gasification process are sparse, and the research that have been conducted have especially emerged in the last several years. Despite the fact that researchers prefer Aspen Plus, there has yet to be a study employing Aspen HYSYS. Furthermore, with the exception of Salaudeen et al. [44]'s work, no study analyzing system performance depending on biochar characteristic has been described. The impact of 10 different woody biochars on gasification performance is extensively examined in this paper. The uniqueness of this study may be considered from two points of view. To the best of our knowledge, although gasifier and/or gasification systems have been modeled using various thermodynamic simulation programs, no model for a CFB gasifier has been developed using the Aspen HYSYS simulation program, which is widely used in the industry. Second, this study was the first to investigate the gasification of different biochar with different operating parameters under steam and CO_2 atmospheres. The result of this research contributes to the determination of suitable operating parameters for biochar gasification under steam/CO_2 atmosphere to achieve the desired syngas production, especially hydrogen generation.

2. Methodology

2.1. Feedstock characterization

Torrefied woody biomass samples were chosen as solid fuel in this study. The proximate and ultimate analysis results, which are required input parameters for gasification simulation, were reviewed for biochar samples produced in various research in the literature. The biochar production process from raw biomass, according to the researchers, involves temperatures ranging from 225° to 320°C and a residence time from 16.5 to 60 min. Table 2 summarizes the proximate and ultimate analysis results for the biochar samples used in the Aspen HYSYS model.

Table 1
Comparison of the current study's findings with those of previous research.

Reference	Materials	Gasification medium	Modeling software	Research context
This study	Various woody biochar samples (10 samples)	Steam and CO_2	Aspen HYSYS	Thermodynamic analysis
AlNouss et al. [21]	Coconut coir pith and its char	Steam	Aspen Plus	Techno-economic analysis
Kraisornkachit et al. [42]	Mangrove tree charcoal	Steam, O_2 and CO_2	Aspen Plus	Thermodynamic analysis
Salaudeen et al. [44]	Hydrochar derived from four fruit wastes	Steam	Aspen Plus	Thermodynamic analysis
Zhang et al. [43]	Pine biomass, biochar, and pyrolysis oil	Steam	Aspen Plus	Techno-economic analysis

The feedstock materials used in the CFB gasifier model are torrefied forms of forest waste and hard/soft woody biomass samples, as indicated in Table 2. Volatile matter and fixed carbon parameters are frequently included in the proximate analysis result. Aspen HYSYS software, unlike Aspen Plus, does not have a specialized library for heterogeneous solid fuels. In other words, Aspen HYSYS does not allow you to specify coal or biomass and calculate its physicochemical parameters. This is another reason why developing a gasification system using Aspen HYSYS is difficult. As a result, the elemental composition of the biochar samples, as well as the ash and moisture content results, are all provided in the simulation model's feed stream. The Van Krevelen diagram is also a method for characterizing solid fuels, particularly for determining their carbonization degree. Solid fuels' membership in a particular class can be observed in the diagram by calculating the H/C and O/C values, and information about their quality can be acquired. The Van Krevelen diagram for biochar samples used in this study is depicted in Fig. 1.

Biomass samples, as is well known, contain high O/C and H/C ratios, indicating that they are solid fuels with low calorific value [51]. The torrefaction process, on the other hand, increases the C content of the fuel while lowering the H and O contents [52]. As a result, the solid fuel's heating value increases as the C-C bonds increase, and it fits into a class similar to coal or coal in terms of carbonization degree. Biochar samples are mostly in the peat grade, as seen in the Fig. 1, but those with a higher degree of carbonization are in the lignite or even coal grade. Teak and melina, the feedstock samples with the highest C and lowest O content, can be classified as lignite and coal, respectively. Furthermore, when compared to other samples, the H content of these biochar samples is low. Camphor, cedar, and hardwood biochars are the specimens spotted near the lignite class inside the peat class. Camphor, cedar, and hardwood biochar samples have H/C ratios of 0.972, 1.038, and 1.114, respectively, and O/C ratios of 0.397, 0.412, and 0.402. Finally, the peat-biomass class comprises the group of five biochar samples. The H/C ratios for stem, spruce, birch, softwood, and pine samples are 1.217, 1.236, 1.235, 1.226, and 1.263, respectively, whereas the O/C ratios are 0.526, 0.488, 0.489, 0.451, and 0.441. These biochar samples, as can be observed, have high H:C and O:C proportions and thus low calorific values.

2.2. Thermodynamic equilibrium modeling

The gasification procedure includes a complex series of chemical reactions, which necessitates the development of mathematical models to describe [53]. These models are critical for analyzing processes, identifying optimal operational conditions, and examining parameters that influence results. Furthermore, mathematical models are rate-based or equilibrium-based expressions that frequently include mass and energy balance calculations. Thermodynamic equilibrium, kinetic, computational fluid dynamics (CFD), and artificial neural network (ANN) and process simulators are some of the most commonly used methods for the modeling of gasification process [54]. CFD and kinetic rate expression models both require the knowledge of reaction and diffusion parameters, as well as longer computation times [55]. Thermodynamic equilibrium models, on the other hand, assume that the reactions have reached an equilibrium state. There are two types of thermodynamic equilibrium models: non-stoichiometric models minimize the Gibbs free energy to form possible reaction products and stoichiometric models minimize the equilibrium constants for specific reactions in the process. Under the same gasification conditions, both modeling approaches should provide identical results. In stoichiometric models, however, all of the reactions that occur during the gasification process must have stoichiometric coefficients, and the equilibrium

Table 2
The characterization of the biochar samples used in this study.

Feedstock Material	Moisture	Ash	C	H	O	N	S
Stem (Norway spruce) [45]	–	0.40[a]	55.20[a]	5.60[a]	38.70[a]	0.10[a]	0.00[a]
Spruce [46]	–	0.14[a]	56.99[b]	5.87[b]	37.07[b]	0.07[b]	0.00[b]
Birch [46]	–	0.13[a]	56.92[b]	5.86[b]	37.13[b]	0.09[b]	0.00[b]
Hardwood [47]	3.70[a]	2.10[a]	61.40[b]	5.70[b]	32.90[b]	0.00[b]	0.00[b]
Softwood [47]	3.90[a]	0.40[a]	58.70[b]	6.00[b]	35.30[b]	0.00[b]	0.00[b]
Cedar [48]	–	2.02[a]	61.02[b]	5.28[b]	33.49[b]	0.22[b]	0.00[b]
Camphor [48]	–	2.54[a]	61.94[b]	5.02[b]	32.81[b]	0.23[b]	0.00[b]
Pine [49]	–	0.30[a]	58.90[a]	6.20[a]	34.60[a]	0.00[a]	0.00[a]
Teak [50]	2.01[c]	2.00[c]	68.70[a]	4.86[a]	23.89[a]	0.34[a]	0.21[a]
Melina [50]	1.15[c]	2.17[c]	75.34[a]	4.02[a]	17.94[a]	0.32[a]	0.21[a]

[a] weight%, as received basis,
[b] weight%, dry basis,
[c] weight%, dry-ash free basis.

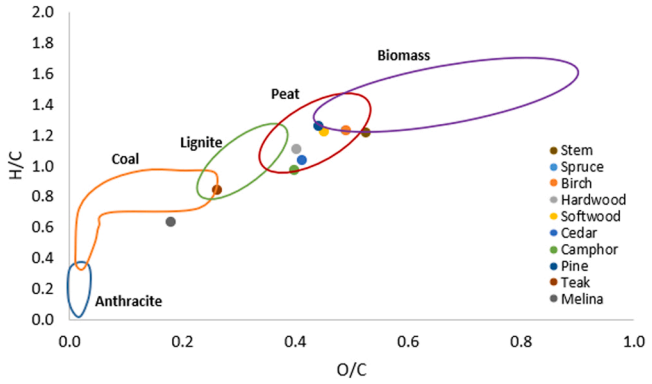

Fig. 1. Characterization of biochar samples by Van Krevelen diagram.

constants should be determined accordingly. Non-stoichiometric models, on the other hand, are based on minimizing Gibbs free energy and are typically a constrained optimization problem solved using the Lagrange multiplier approach [56]. The biochar gasification system was modeled using "RGIBBS" reactors in this work. The "RGIBBS" reactor module predicts equilibrium using the Gibbs free energy minimization principle following phase separation in the absence of defining the chemical reaction formula's measurement coefficient [57]. When the gasification reactions achieve equilibrium, the system's Gibbs free energy is minimized, as given below:

$$G^t = \sum_{i=1}^{N} n_i \mu_i \quad (1)$$

where the number of moles and chemical potential of species i are represented by n_i and μ_i respectively.

$$\mu_i = G_i^m + RTln(f_i/f_i^m) \quad (2)$$

where G_i^m is the universal standard Gibbs free energy, whose value is independent of the type of gas and is associated only to the unit. The gas constant is R, the temperature is T, and the fugacity and standard fugacity of species i are f_i and f_i^m respectively. μ_i can be written as follows at standard pressure:

$$\mu_i = \Delta G_{f,i}^m + RTln(x_i) \quad (3)$$

where x_i denotes the molar fraction of gas species i, and $\Delta G_{f,i}^m$ signifies the standard Gibbs free energy for the formation of species i. The value of n_i for which the system's total Gibbs free energy is reduced can be determined by substituting Eq. (3) into Eq. (1) using the Lagrange multiplier approach.

$$(\partial L/\partial n_i) = \Delta G_{f,i}^m + n_i RTln(n_i/n_{total}) + \sum_{j=1}^{k} \lambda_j a_{ij} = 0 \quad (4)$$

where a_{ij} is the number of atoms of the j_{th} element in a mole of the i_{th} species, and L and λ_j are the Lagrange function and Lagrange multiplier, respectively. Eq. (4) generates a set of iteratively solveable nonlinear equations.

2.3. Development of the CFB gasifier model

Simulation programs can be used to design and optimize physical, chemical, and biological systems. Aspen HYSYS is a process simulator that optimizes process parameters while reducing operational time and expenses. A CFB gasifier steady-state equilibrium model for the biochar gasification process was developed in Aspen HYSYS V11. If an appropriate CFB gasifier model can be established, an investigation of the various syngas characteristics can be conducted using the created model and a case study module. AspenTech's user manual [58] recommended using the Soave-Redlich-Kwong (SRK) equation of state for calculating physical properties of components. Only the major parts of biochar gasification have been considered, with certain assumptions, due to the complicated chemical pathways throughout a gasification procedure. The simulation was created based on a number of different assumptions:

- A steady-state, isothermal process was used to operate the whole gasification process.
- Tar and other heavy hydrocarbons were not included in the syngas content.
- Chemical equilibrium is immediately reached since all reactions are rapid.
- Char is made up entirely of carbon.
- Ash is a non-reactive substance.
- H_2S and HCl have been produced from all sulfur and chlorine compounds.
- Pressure drops were neglected while the reactors were operated at atmospheric pressure.

Fig. 2 depicts the process flowsheet diagram of steam/CO_2 gasification of biochar samples in the Aspen HYSYS.

The input material streams are the gasification agents "*Steam*" and "*CO_2*" as well as the fuel stream "*Biochar*". The "*Steam*" stream contains 200 °C pure water, the "*CO_2*" stream contains pure CO_2, and the "*Biochar*" stream contains the solid fuel's elemental composition and proximate analysis data. The physicochemical characteristics of biochar samples on as received basis. Moreover, the component splitter block "*X-103*" separates the ash from the biochar input stream. As a consequence, the "*Fuel*" stream turns into a dry-ash-free basis. Since the Aspen HYSYS component library does not include an inert solid substance like sand, this separation is necessary. Also, the synergistic effects of the ash component were ignored in the CFB gasification simulation, and it was assumed to be completely inert. Other researchers have made the same assumption [29,59,60]. In summary, the cyclone equipment that

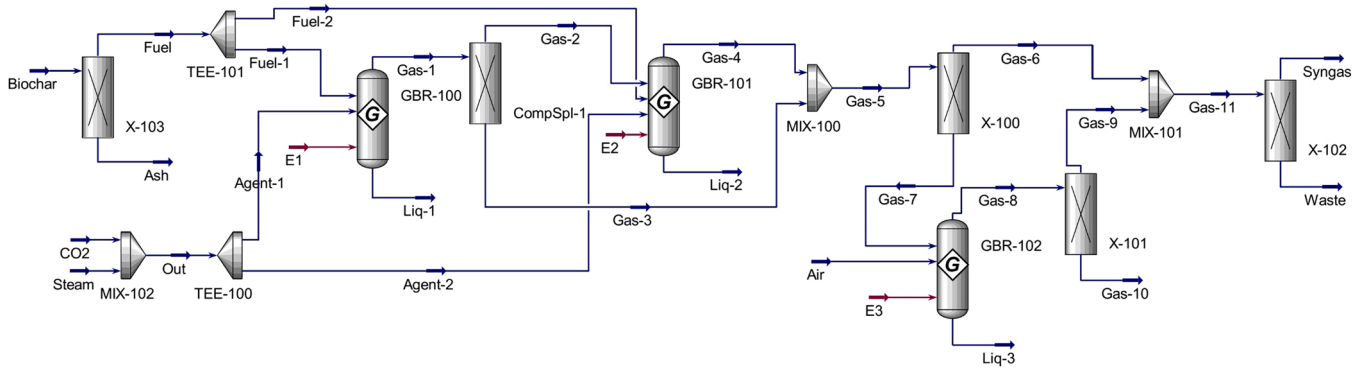

Fig. 2. Process flow diagram for steam/CO_2 gasification in Aspen HYSYS software.

separates the ash is the "*X*-103" unit block in the simulation model. In the "*MIX-102*" unit block, steam and CO_2 feed streams merge, then continue to the "*GBR-100*" and "*GBR-101*" reactors, dividing in a specific mass fraction in the "*TEE-100*" unit block. Similarly, in the "*TEE-101*" unit block, the "*Fuel*" stream is divided into a certain mass fraction and sent to the Gibbs reactors, where all of the gasification reactions take place. In general, CFB gasification procedure takes place in Gibbs reactors "*GBR-100*", "*GBR-101*", and "*GBR-102*". The "*GBR-100*" reactor conducts low-temperature reactions, whereas the "*GBR-101*" unit block performs high-temperature reactions, primarily reduction reactions. Additionally, in the "*GBR-102*" reactor, combustion processes occur. The objective of developing such a reactor distribution is to get a realistic syngas composition and create a CFB gasifier simulation that fits the experimental results. If a single temperature unit block is employed, such as the "*GBR-101*" reactor at 800 °C, all components will achieve equilibrium at 800 °C, and components decomposed at high temperatures, such as methane, will be difficult to detect in the syngas. Table 3 summarizes the details of the CFB gasifier model's unit blocks.

A unique CFB gasifier design is based on the split fractions allocated to each unit block. Changes in these split fractions have an impact on the composition of syngas and other physicochemical features, or in other words, they modify the design parameters. In other words, while thermodynamic equilibrium-based models have been developed for various types of gasifiers in the literature, the type and number of unit blocks (such as component splitter and tee) as well as the values assigned to these unit blocks (such as split ratio) distinguish the model in this study as a CFB gasifier. The model validation section discusses the comparability of the CFB model created in this work with the experimentally operated CFB gasifier output.

The split fractions were adjusted until syngas characteristics were obtained that were consistent with the literature results. "*CompSpl-1*" isolates components that should not react in the Gibbs reactor "*GBR-101*". Moreover, the "*X-100*" unit block is responsible for separating the components that will be delivered to the combustion reactor. This substantially resolves the issue of high H_2 and CO concentrations in the syngas composition. Furthermore, if unconverted carbon is detected, "*X-100*" assists the modeling of solid-state combustion process. Also, the "*Air*" flow into the "*GBR-102*" reactor is rather significant. Since a complete combustion process must be completed, the volume of air in this stream is excessive. The "*X-101*" unit block, on the other hand, separates the high quantities of O_2 and N_2 provided by the "*Air*" stream because it produces a significant concentration change in the syngas composition. The final component splitter block before syngas production is "*X-102*", which separates components such as H_2O and N_2. Some authors provide syngas compositions on dry or dry-nitrogen-free basis. This unit block is quite important for the model validation section, since it is required to achieve results that are consistent with the literature. The main homogeneous and heterogeneous reactions involved in biochar gasification are listed below:

- Boudouard reaction: $C + CO_2 \leftrightarrow 2CO$ (+172 MJ/kmol)
- Water-gas shift reaction: $CO + H_2O \leftrightarrow CO_2 + H_2$ (−41 MJ/kmol)
- Steam-methane reforming reaction: $CH_4 + H_2O \leftrightarrow CO + 3\ H_2$ (+206 MJ/kmol)
- Partial combustion: $C + 0.5\ O_2 \rightarrow CO$ (−111 MJ/kmol)
- Complete combustion: $C + O_2 \rightarrow CO_2$ (−393 MJ/kmol)
- Water-gas reaction: $C + H_2O \leftrightarrow CO + H_2$ (+131 MJ/kmol)
- Hydrogenation: $C + 2\ H_2 \leftrightarrow CH_4$ (−75 MJ/kmol)

Table 3
Descriptions of the ASPEN HYSYS unit blocks.

Block ID	Aspen HYSYS UnitOPS	Function
GBR-100 (400 °C) GBR-101 (800 °C) GBR-102 (1000 °C)	Gibbs reactor	The Gibbs free energy minimization method is used to simulate reactions between reactants and determine possible products.
TEE-100	Tee	Splits the gasification agent as 20 % wt. into Agent-1 % and 80 % wt. into Agent-2.
TEE-101	Tee	Splits the biochar feed as 5 % wt. into GBR-100 % and 95 % wt. into GBR-101.
CompSpl-1	Component splitter	Separates the methane, hydrogen, carbon monoxide and oxygen in Gas-1 stream.
X-100	Component splitter	Separates the methane (50 % vol.), ethane (50 % vol.), propane (50 % vol.), water (100 % vol.), hydrogen (47 % vol.), carbon dioxide (100 % vol.), sulphur (100 % vol.), carbon monoxide (10 % vol.) and carbon (100 % wt.) in Gas-5 stream.
X-101	Component splitter	Separates the nitrogen and oxygen in Gas-8 stream.
X-102	Component splitter	Separates the undesired components (water, nitrogen, etc.) in Gas-11 stream.
X-103	Component splitter	Separates the ash content in Biochar stream.
MIX-100 MIX-101 MIX-102	Mixer	It combines the input streams into a single output stream.

3. Results

3.1. Model validation

The novel CFB gasifier model's reliability was assessed by comparing its syngas composition to that of existing empirical findings in the literature. There were input variables including feedstock material characteristics, gasifier temperature, gasification agent flow rates and solid fuel flow rates used in the simulation of the gasification process under identical experimental circumstances. Fig. 3 shows a comparison between experimental syngas compositions (with biomass [61], biochar

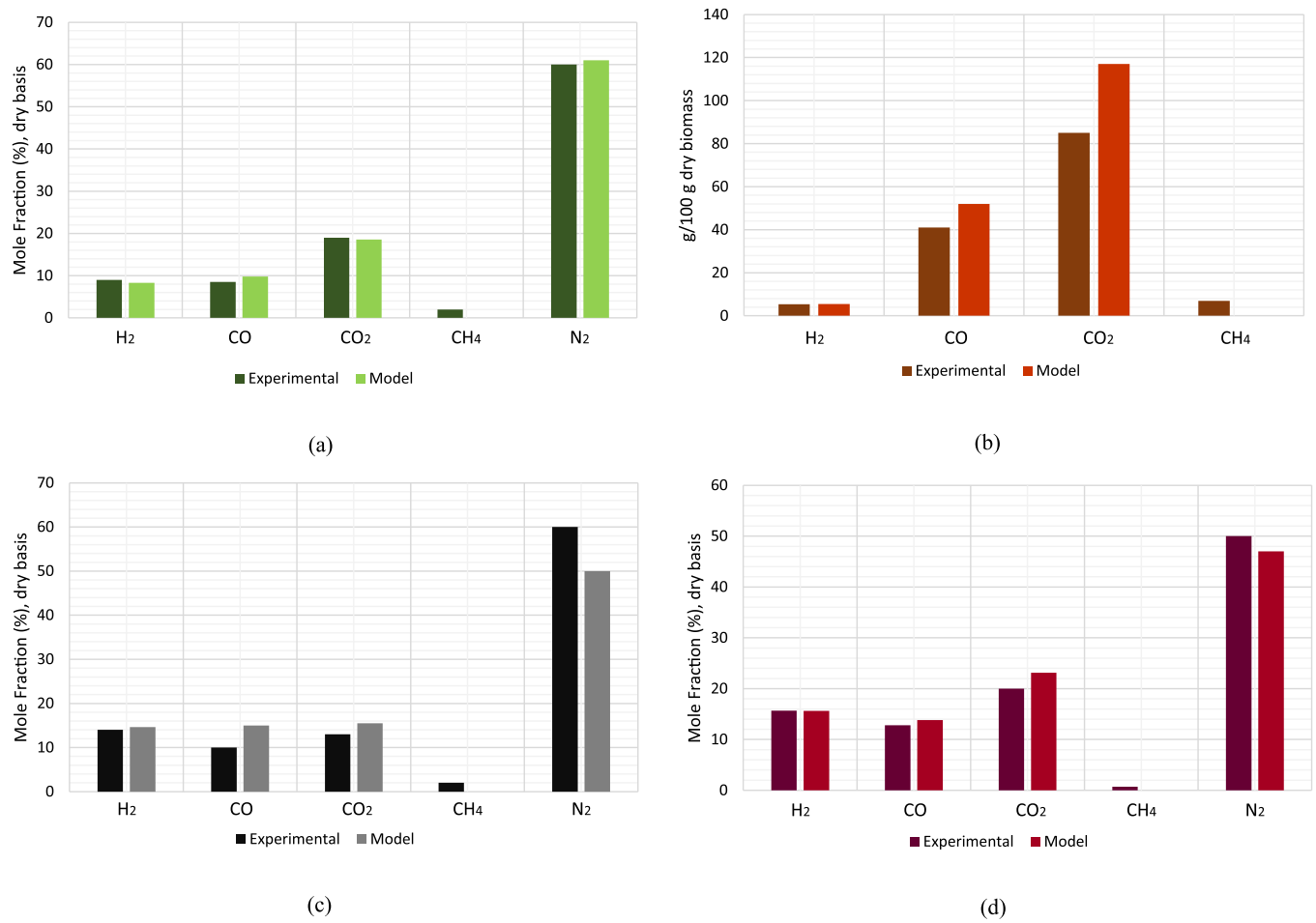

Fig. 3. Literature and developed model comparison of syngas composition. (a) Biomass [61], (b) Biochar [62], (c) Coal [63], (d) Co-gasification [64].

[62], coal [63] and coal/biomass blend [64] samples) and the results of a newly designed CFB gasifier model.

Before continuing parametric work on the CFB gasifier, it is crucial that the simulation model be verified. Because an unreliable model can't be trusted, and correct conclusions can't be considered. Validation procedures were done on four different types of solid fuels since the fuels used in this study were biochar samples. Biochar is positioned somewhere between biomass and coal in terms of carbonization degree, therefore the newly developed CFB gasification model has been validated using biomass, coal, co-gasification, and biochar gasification processes. Study validated with biomass sample under air atmosphere is reported by García-Ibañez et al. [61], study validated with biochar sample under O_2/steam gasification atmosphere is reported by Berrueco et al. [62], study validated with coal sample under air/steam atmosphere is reported by Duan et al. [63], and study validated with coal/-biomass sample under oxygen/steam atmosphere is reported by Li et al. [64]. When examining at the findings in Fig. 3, it's noticeable that the syngas composition provided by the CFB model fits the experimental results. For all four solid fuels, the H_2 content estimation is quite accurate. Estimation of the CH_4 gas percentage is difficult for the thermodynamic equilibrium systems due to the conversion of hydrocarbons into H_2, CO, and CO_2. The CH_4 compositions deviate from the experimental values due to the CFB model's independence from the design parameters, negligence of reaction kinetics and fluid dynamics, together with the virtually infinite residence time in the reactors. This problem has been highlighted by other researchers and has been observed in various equilibrium models [65,66]. Furthermore, when the results of the biochar sample (Fig. 3.b) are compared to the other samples, it can be seen that the deviation is slightly greater. It is undeniable, however, the unit in which the comparison is performed has an influence. The authors reported "*The main components of the gas are H_2 (30–40 % db. volume), CO_2 (30–37 db. volume), CO (18–24 % db. volume), and CH_4 (4–12 % db. volume)*" [62]. Further, the results of the CFB gasifier model are H_2 (37.15 % db. volume), CO_2 (36.87 % db. volume), CO (25.67 % db. volume) and CH_4 (0 % db. volume). These values are within the range of the researchers' calculations. In conclusion, when the CFB gasifier model is run with the identical operating conditions and input variables, the results successfully approximate experimental investigations. The CFB gasifier model is capable of simulating the gasification process, although the four solid fuels used had different physicochemical properties and the experiments were conducted under different operating conditions.

3.2. Parametric study

A novel CFB gasifier model was used to investigate the effect of CO_2/biochar ratio, gasifier temperature, gasifier pressure and steam/biochar ratio on syngas composition and HHV during biochar gasification. This set of parametric tests included one variable that was altered while the others remained the same. Furthermore, the gasifier's parametric studies are examined by altering the GBR-101 reactor's operating settings. Because, as explained in Section 3.1, the GBR-100 and GBR-102 reactors are modules that deal with low and high temperature thermochemical processes, with fixed operational parameters assigned to provide a suitable syngas composition and to mimic different thermochemical phenomena in the gasifier. The temperature of the gasifier was adjusted between 600 and 1000 °C, the steam/biochar - CO_2/biochar ratios were varied between 0 and 2.0, and the pressure of

the gasification process was changed between 1 and 16 bar.

3.2.1. Effect of gasifier temperature on the syngas composition

The gasification temperature has a significant impact on the performance of biochar gasification system since it is directly related to the composition of gas generated. According to Le Chatelier's principle, increasing the temperature promotes endothermic reactions whereas shifts the chemical equilibrium in exothermic reactions to the side of the reactants [67]. Fig. 4 depicts the effect of gasifier temperature on syngas composition.

When the temperature rises, the syngas composition of all biochar samples changes in the same manner; however, the yields differ. The molar concentration of H_2 increases at first, then starts to decline. This increasing and decreasing trend can be seen in all types of biochar samples, with the H_2 fraction ranging from 20 % to 26 %. Furthermore, the highest fraction of the H_2 component was recorded between 650 and 700 °C for all biochar samples. Additionally, the melina biochar produces the lowest H_2 concentration in syngas, whereas the pine biochar produces the maximum H_2 concentration in syngas. The sample with the lowest O/C and H/C values is melina, whereas the sample with the highest H/C value is pine. On the other hand, Teak biochar has a different trend from other biochars, because the change of the distribution of chemical content in elemental analysis and proximate analysis can cause a difference in the trend of hydrogen formation in Teak biochar. The increase in H content in the biochar sample have led the H_2 fraction in the syngas to rise, according to this finding. Moreover, the H_2 fraction in the syngas produced through gasification of biochar samples, which is closer to the biomass class in the Van Krevelen diagram, is greater. This result is also consistent with the conclusion that biomass, when compared to other solid fuels, potentially provide higher H_2 yields in the steam gasification process [68]. Endothermic processes in the solid gas phase, such as steam-methane reforming and water-gas reactions, could be responsible for the increase in H_2 concentration at high temperatures. Furthermore, when the gasifier temperature increased, a negative relationship between CO and CO_2 fractions was observed. The CO_2 fraction decreased from 46 % to 30 %, whereas the CO fraction increased from 25 % to 42 %. The shift in concentrations of these substances in the syngas can be attributed mostly to the Boudouard reaction's equilibrium state. Also, up to 700 °C, the increase in CO fraction and decrease in CO_2 fraction for all biochar samples is remarkable, whereas the change is slower at higher temperatures. Teak and melina biochar samples were found to have the greatest CO contents (higher than 44 % at 800 °C). Similarly, teak and melina biochar samples had the lowest CO_2 contents (lower than 28 % at 800 °C). These two biochar samples have one common characteristic: they are solid fuels with the highest carbonization degrees. That is, the solid fuel's high C content shifted the Boudouard reaction toward the products, improving CO yield. Moreover, as the temperature increases, the concentration of CH_4 decreases fast, and there is almost no CH_4 in the syngas composition beyond 800 °C. At high temperatures, the forward reaction of steam-methane reforming achieves chemical equilibrium, resulting in CH_4 decomposition [69]. Melina and teak biochar samples were found to have the greatest fraction of CH_4 in syngas. As a result, increasing the carbonization degree has a positive impact on the CH_4 yield.

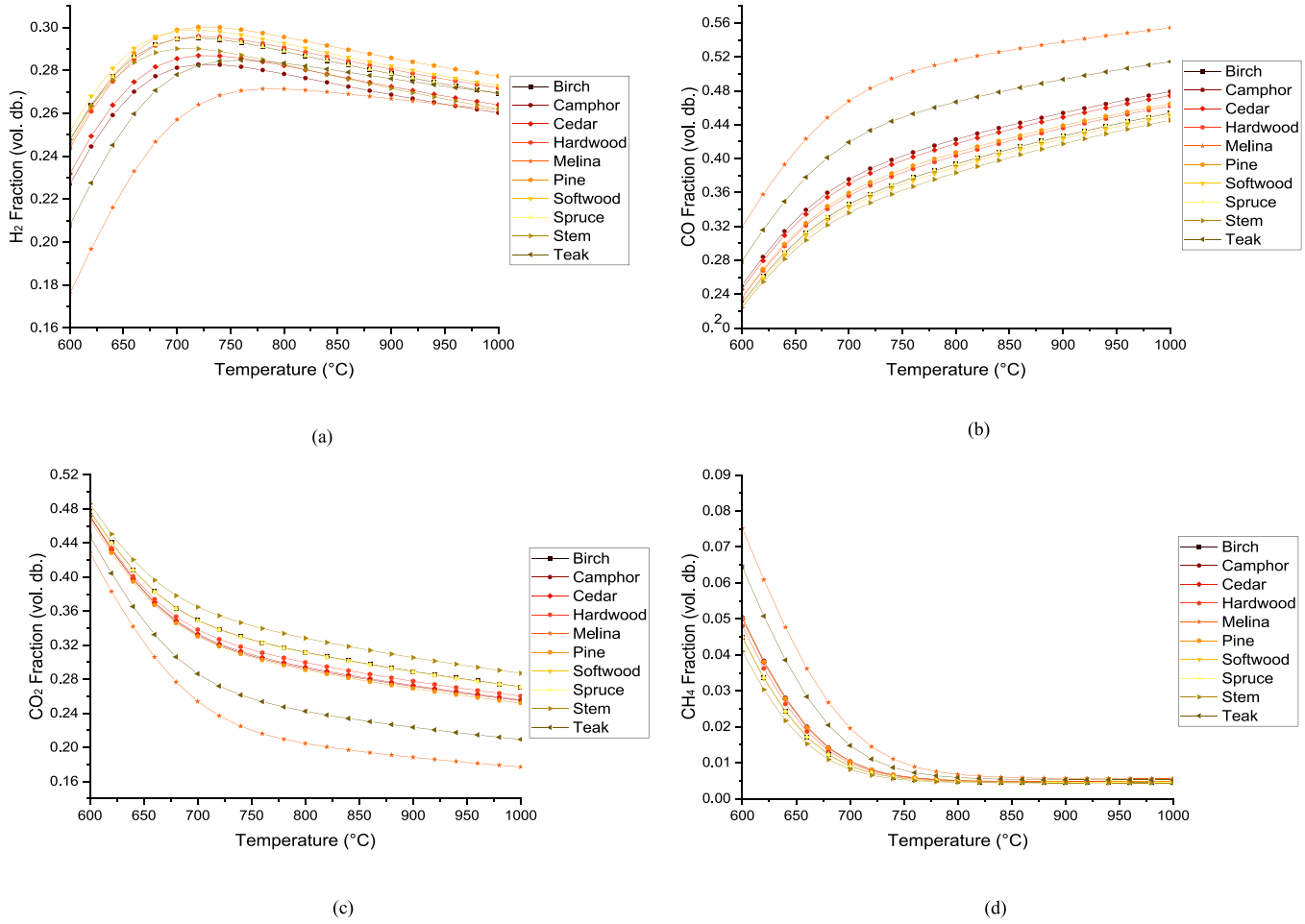

Fig. 4. Effect of gasifier temperature on the syngas composition (Gasifier pressure: 1 bar, Steam/biochar ratio: 1.0, CO_2/biochar ratio: 1.0), (a) H_2, (b) CO, (c) CO_2, (d) CH_4.

3.2.2. Effect of gasifier temperature on the syngas HHV

The calorific value of a fuel is usually represented as the HHV. The maximum possible energy released after complete oxidation of a fuel unit is referred to as the HHV. This necessitates the condensing and cooling of the thermal energy recovered from all combustion products [70]. Therefore, determining the syngas HHV at the end of the gasification process is crucial. The HHV of syngas could be accessed in the stream characteristics section of the Aspen HYSYS simulator. The impact of gasifier temperature on syngas HHV is seen in Fig. 5.

When the behavior of syngas HHV was examined between 600 and 1000 °C, it was observed that the HHV of syngas was constantly increasing. The increased CO and H_2 content is the rationale for the increasing trend with increasing gasification temperature. Other researchers have observed identical results [71,72]. Moreover, beyond 700 °C, a change in the slope of the HHV can be detected owing to the reduction in increment in CO concentration. Thus, the CO concentration plays a significant role in the syngas HHV characteristics. Teak and melina biochar samples stand out as the syngas with the highest HHV. As the gasifier temperature raised from 600 °C to 1000 °C, the syngas HHV increased from approximately 200 MJ/kmol to 225 MJ/kmol. As a result, increasing the degree of carbonization for solid fuel has a favorable influence on syngas HHV. Biochar samples close the biomass class, on the other hand, provided syngas with low HHV.

3.2.3. Effect of steam/biochar ratio on the syngas composition

The proportion of steam entering the gasifier to biochar supplied to the gasifier is defined as the steam to biochar ratio. One of the essential factors, in addition to determining the appropriate gasification temperature, is selecting the atmosphere/solid fuel ratio. Because, like the temperature parameter, the forward/reverse rate of the equilibrium reactions is affected by an increase in the partial pressure of steam in the reactor. Fig. 6 illustrates the effect of the steam/biochar ratio on syngas composition.

Due to heterogeneous char-steam reactions, the H_2 fraction in the syngas increases as the steam/biochar ratio rises. Furthermore, an increase in H_2O promotes the forward reaction of the water-gas shift, resulting in a larger H_2 and CO_2 concentration [73]. Also, constant H_2O supply boosts CH_4 degradation via the steam-methane reforming forward reaction. With a rising H_2O concentration, the partial pressure in the gasifier increases, which stimulates forward water-gas, water-gas shift, and steam reforming reactions [74]. Therefore, for all biochar samples, the H_2 fraction in the syngas composition increased as the steam/biochar ratio increased. The rate of growth in the H_2 fraction, on the other hand, is strongly associated with the biochar sample's physicochemical characteristics. Increasing the carbonization degree of a solid fuel sample delays the point at which the rate of H_2 concentration growth slows. The steam/biochar ratio values for teak and melina, the biochar samples with the lowest H/C and O/C ratios, are about 0.35 and 0.45 at this point, respectively. While the steam/biochar ratio value for camphor and cedar with a low degree of carbonization is about 0.30 at this point, the steam/biochar ratio value for other biochar samples may be lower than 0.20. As the steam/biochar ratio increases, there is also an increase in CO_2 with a significant decrease in CO fraction. The forward shift of the water-gas shift reaction clarifies this behavior. Furthermore, an increase in H_2O concentration in the gasifier accelerates the steam-methane reforming reaction, resulting in a large reduction in CH_4 concentration. When these observations are evaluated considering the characteristics of biochar samples, melina and teak stand out as the materials with the highest CO content in any steam/biochar ratio. When the steam/biochar ratio exceeds 0.4, the CO content for these samples decreases dramatically. If the steam/biochar ratio is 0.3 or less for other biochar samples, the CO content decreases rapidly. Moreover, methane gas can be obtained with fuels that have high C/O and C/H values at low steam/biochar ratios and low gasification temperatures. At a steam/-biochar ratio of 0.25, CH_4 with a fraction of more than 8 % in syngas can be obtained for the melina sample, while at a steam/biochar ratio of 0.10, CH_4 with a fraction of more than 7 % in syngas can be obtained for the teak sample. In summary, the high C content of the solid fuel improves CH_4 yield, but it also raises the required steam/biochar ratio.

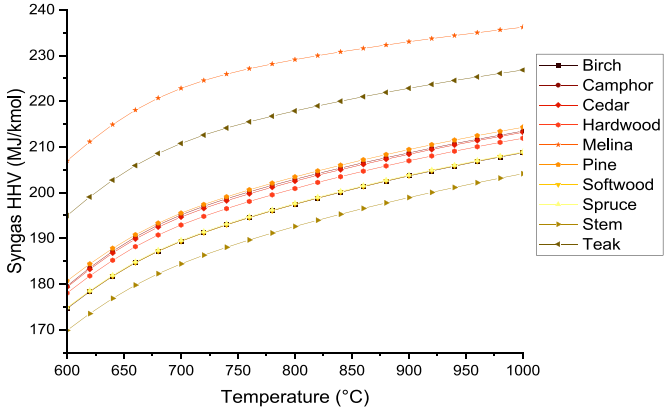

Fig. 5. Effect of gasifier temperature on the syngas HHV (Gasifier pressure: 1 bar, Steam/biochar ratio: 1.0, CO_2/biochar ratio: 1.0).

3.2.4. Effect of steam/biochar ratio on the syngas HHV

The steam/biochar ratio has a major effect on the chemical composition of syngas, which also has an impact on the HHV of syngas. The effect of the steam/biochar ratio on the syngas HHV is demonstrated in Fig. 7. The syngas HHV was diminished when the steam/biochar ratio was increased, as seen in Fig. 7. Despite the steady increase in H_2 fraction, CO_2 enrichment and CO depletion consistently reduced the HHV of syngas. Furthermore, when the steam/biochar ratio increased, the CO_2 fraction grown massively, resulting in a continual decrease of syngas HHV. Teak and melina were identified as the biochar samples that resulted in greater HHV syngas production. HHV decreased from 298 MJ/kmol to 196 MJ/kmol for melina and from 301 MJ/kmol to 188 MJ/kg for olive pits when the steam/biochar ratio increased from 0.0 to 2.0. The HHV decreased on average from 265 MJ/kmol to 175 MJ/kmol for the other biochar samples.

In brief, as the concentration of combustible gas components in the syngas decreased with rising H_2O concentration, the heating value of the produced gas decreased. Other authors have observed similar phenomena [57,75]. When the heating quality of syngas is assessed in terms of biochar properties, it is observed that samples with a high C content produce syngas with a high HHV.

3.2.5. Effect of CO_2/biochar ratio on the syngas composition

The process model was simulated by varying the CO_2/biochar ratio between 0.0 and 2.0 at constant gasifier temperature and steam/biochar ratio to evaluate the impact of the CO_2/biochar ratio on the syngas composition. The change in the syngas composition with regard to the CO_2/biochar ratio is visualized in Fig. 8.

The H_2 and CH_4 concentrations reduce while the CO_2 fraction increases as the CO_2/biochar ratio increases for all biochar samples. CO is the only component that has different properties. After a particular CO_2/biochar ratio value, the CO fraction in syngas rises, but then decreases. The Boudouard reaction shifting forward in response to increasing CO_2 concentrations in the gasifier can explain this phenomenon, but the inevitable increment in the CO_2 fraction in the syngas at extreme concentrations. Melina had a CO_2/biochar ratio of 0.5 with the greatest CO concentration, while teak had a CO_2/biochar ratio of 0.6 with the highest CO concentration. The CO_2/biochar ratio at which the highest CO fraction was achieved was about 0.9–1.0 for samples with high O/C and H/C values, such as birch, pine, and spruce. As a consequence, increasing the C content of solid fuels lowers the quantity of CO_2 necessary to produce CO at its maximum concentration. Furthermore, when the carbonization degree of the solid fuel increases, syngas with

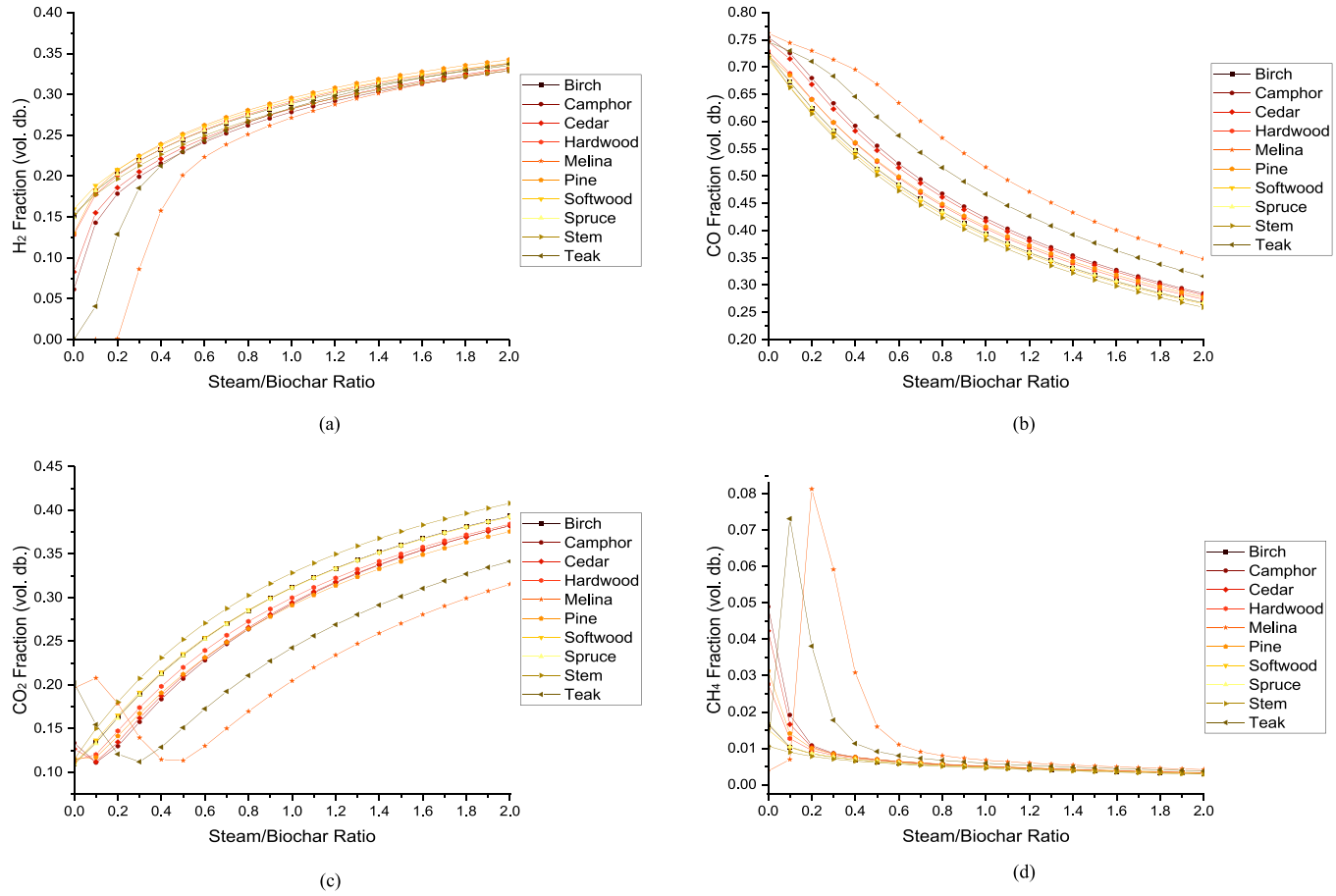

Fig. 6. Effect of steam/biochar ratio on the syngas composition (Gasifier temperature: 800 °C, Gasifier pressure:1 bar, CO_2/biochar ratio: 1.0), (a) H_2, (b) CO, (c) CO_2, (d) CH_4.

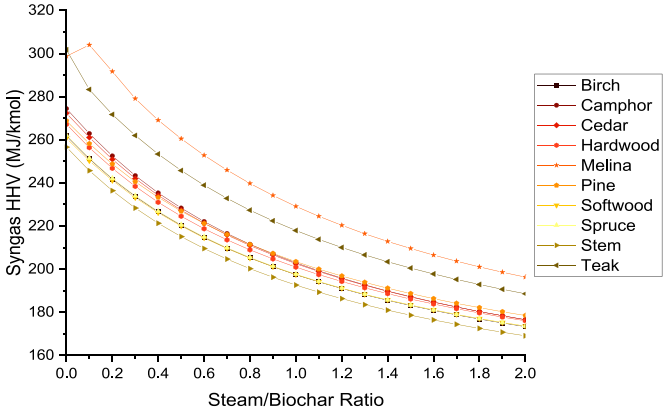

Fig. 7. Effect of steam/biochar ratio on the syngas HHV (Gasifier temperature: 800 °C, Gasifier pressure:1 bar, CO_2/biochar ratio: 1.0).

high CO and CH_4 concentrations but low H_2 and CO_2 concentrations can be synthesized.

3.2.6. *Effect of CO_2/biochar ratio on the syngas HHV*

The process model was simulated by varying the CO_2/biochar ratio between 0.0 and 2.0 at constant gasifier temperature and steam/biochar ratio to investigate the impact of the CO_2/biochar ratio on the syngas HHV. The change in the syngas HHV with regard to the CO_2/biochar ratio is demonstrated in Fig. 9. The syngas HHV has been steadily decreasing as the CO_2/biochar ratio has increased. As the amount of supplied CO_2 increased, the concentration of beneficial gases such as H_2 and CH_4 decrease, while the concentration of CO_2 gas increased. Moreover, the CO increment at low CO_2/biochar ratios was not substantial, and there was no influence on syngas HHV. When the CO_2/biochar ratio was 0.0, the CO fraction for the cedar sample was 40.83 %, and when the CO_2/biochar ratio was 0.7, it was 41.86 %. The H_2 fraction, on the other hand, decreased from 39.97 % to 31.17 % for the same biochar sample and CO_2/biochar ratio change, meanwhile the CO_2 fraction increased from 18.38 % to 26.30 %. Additionally, if the CH_4 concentration is not considerable, it is possible to conclude that it has no influence on syngas HHV.

As a result, increasing the quantity of CO_2 supplied into the reactor resulted in a decrease in syngas HHV. When the heating quality of syngas is evaluated considering biochar characteristics, samples with a high C/O and C/H ratio provide syngas with a high HHV. For instance, the syngas HHV for the softwood sample was 197.46 MJ/kmol and the syngas HHV for the teak sample was 217.89 MJ/kmol, when the CO_2/biochar ratio was 1.0.

3.2.7. *Effect of gasifier pressure on the syngas composition*

Gasifier pressure is an another crucial operating parameter that has a significant influence on the performance of the gasification process. The equilibrium states of the gasification reactions are greatly influenced by the gasifier pressure. The gasification pressure was varied from 1 to 16 bar, and the syngas composition is demonstrated in Fig. 10.

The steam/biochar and CO_2/biochar ratio were held constant at 1, and gasifier temperature was adjusted as 800 °C. With respect to Le Chatelier's principle, a rise in pressure shifts an equilibrium state to the reaction side with the lower moles of gas. Therefore, an enhancement in

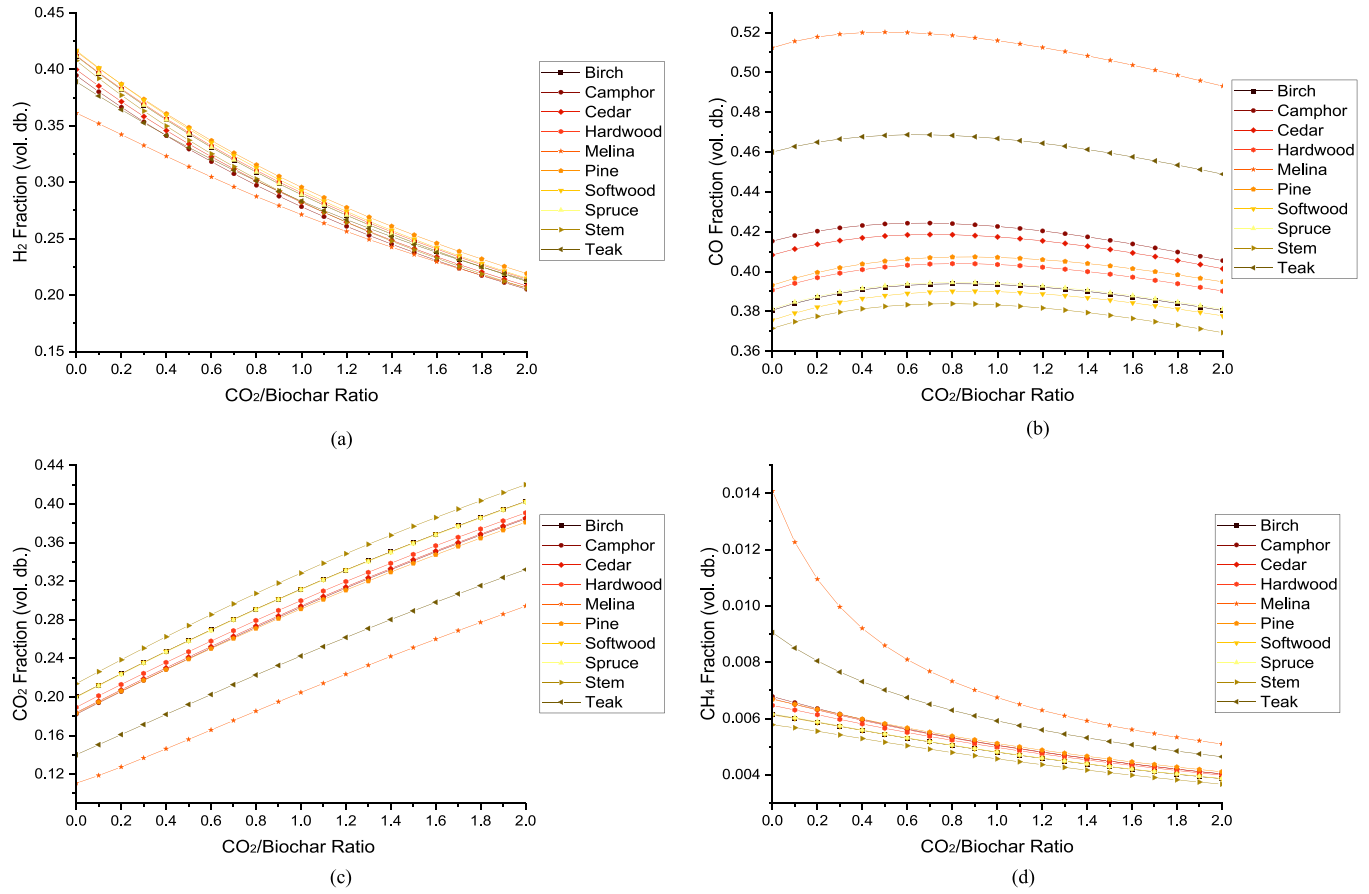

Fig. 8. Effect of CO_2/biochar ratio on the syngas composition (Gasifier temperature: 800 °C, Gasifier pressure:1 bar, Steam/biochar ratio: 1.0), (a) H_2, (b) CO, (c) CO_2, (d) CH_4.

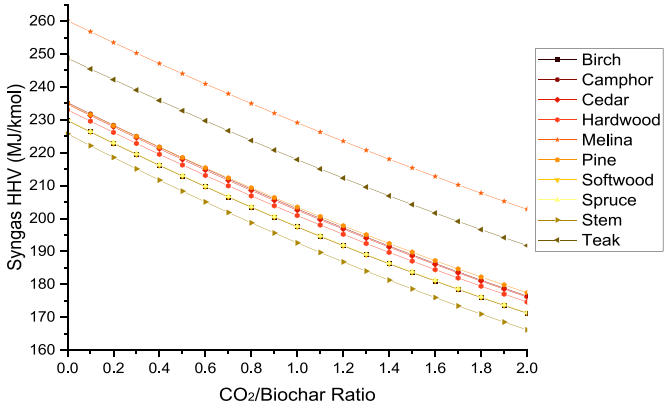

Fig. 9. Effect of CO_2/biochar ratio on the syngas HHV (Gasifier temperature: 800 °C, Gasifier pressure:1 bar, Steam/biochar ratio: 1.0).

pressure shifted equilibrium to the side of the reaction with the higher number of moles of gas and pressure had a significant impact on the syngas composition, as shown in Fig. 10.

Enhancing the gasifier pressure impacted the steam-methane reforming and hydrogenation reactions because their equilibrium states shift to the side that has lower moles of gas. Thus, the mole fraction of CH_4 increased between 3.0 % and 5.5 % for each feedstock with the pressure because the hydrogenation reaction and the reverse of the steam-methane reforming reaction led to more CH_4 production. In addition, mole fraction of H_2 diminished as gasifier pressure increases, and at 1 bar, all feedstocks yield the highest H_2 mole fraction as indicated in the Fig. 10.a. In the case of Melina biochar gasification, the mole fraction of H_2 reduced by around 9.5 %, which was the highest drop in the mole fraction of H_2, with rising pressure from 1 to 16 bar. The decreased H_2 concentration can be explained by hydrogenation, reverse water-gas and reverse steam-methane reforming reactions. The water-gas shift process, on the other hand, is unaffected by pressure changes and hence does not contribute to the change in the H_2 fraction. Increment of the gasifier pressure enhanced the mole fraction of CO_2 while decreasing the mole fraction of CO due to the Boudouard reaction. In addition, the reduction of CO concentration due to the increased gasifier pressure can be explained by reverse steam-methane reforming, partial combustion, and water-gas reactions. In specifically, in the case of Melina biochar gasification, the highest increase and decrease in CO_2 (14.1 %) and CO (10.1 %) mole fractions, respectively, were observed. In short, with increasing gasification pressure, only the fraction of CH_4 among the favorable gases increased, while the fractions of CO and H_2 decreased. Similar to our results, other researchers reported that increasing the gasification pressure decreased the proportions of CO and H_2, while the proportions of CO_2 and CH_4 increased [32,33,44,76–78].

3.2.8. *Effect of gasifier pressure on the syngas HHV*

HHV of syngas was examined with respect to gasifier pressure. To conduct the parametric study the ratios of steam/biochar and CO_2/biochar were set to 1, and the gasifier temperature was set at 800 °C. The impact of gasifier pressure on the HHV of syngas for 10 biochar samples is represented in Fig. 11.

As illustrated in Fig. 11, the syngas HHV continually decreased with the pressure increase because the concentration of beneficial gases such as H_2 and CO decreased while the concentration of undesired gases like CO_2 increased with the pressure. The increase in mole fraction of CH_4

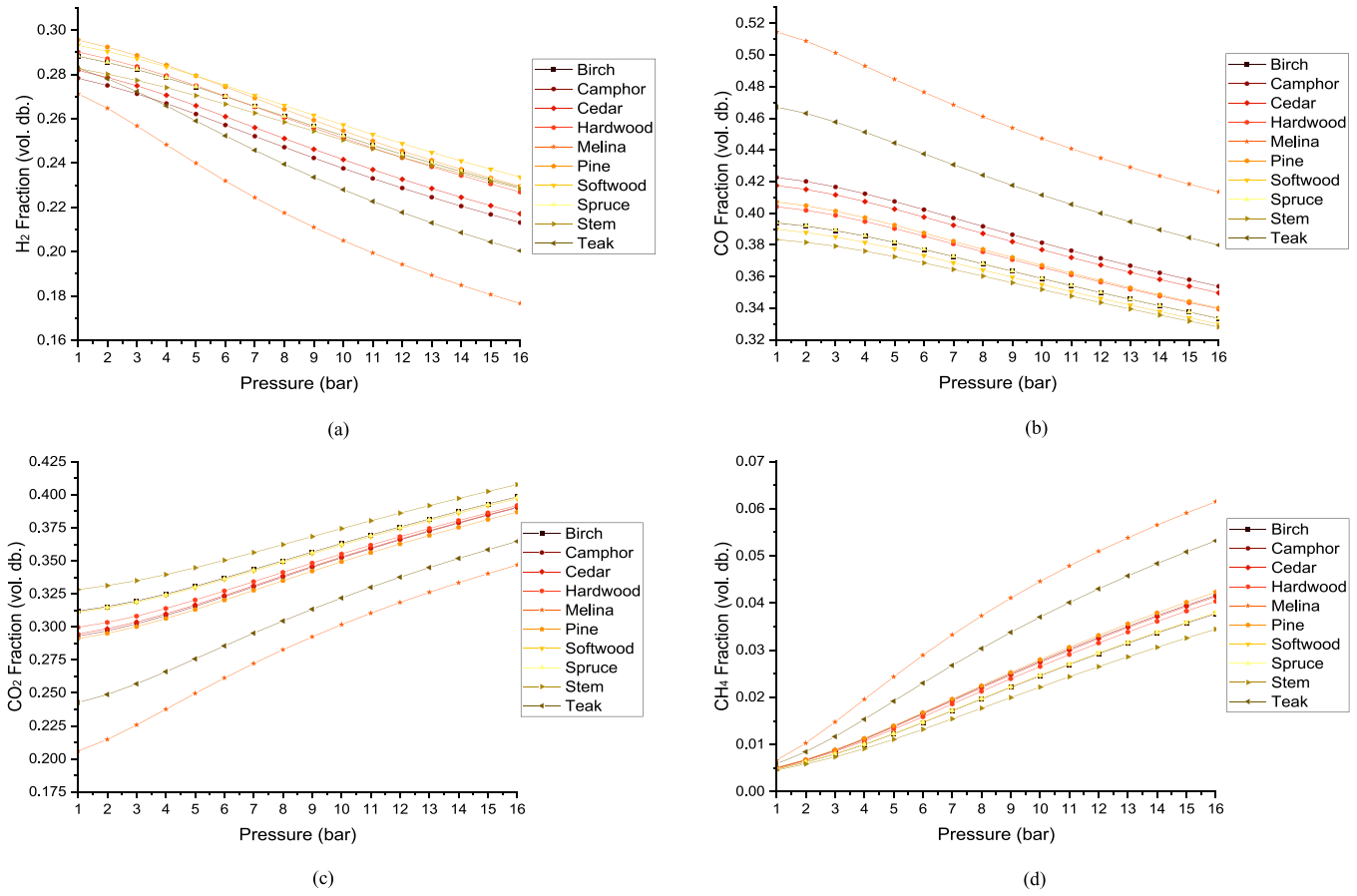

Fig. 10. Effect of gasifier pressure on the syngas composition (Gasifier Temperature: 800 °C, Steam/biochar ratio: 1.0, CO_2/biochar ratio: 1.0), (a) H_2, (b) CO, (c) CO_2, (d) CH_4.

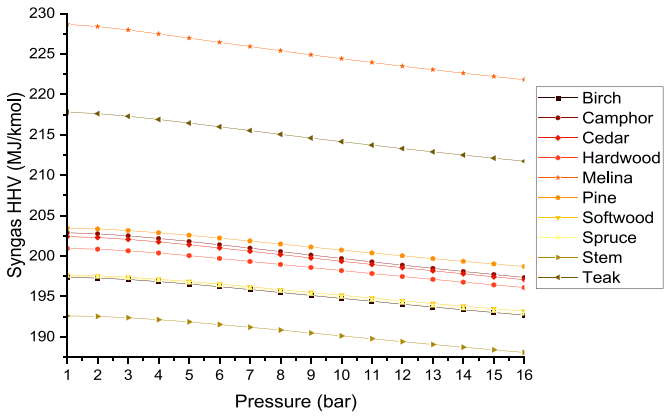

Fig. 11. Effect of gasifier pressure on the syngas HHV (Gasifier temperature: 800 °C, Steam/biochar ratio: 1.0, CO_2/biochar ratio: 1.0).

(3.0–5.5 %) as a valuable gas couldn't show an adequate influence on the syngas HHV to compensate the drop of H_2 (5.4–9.5 %) and CO (5.5–10.1 %). When the heating quality of syngas is examined with biochar properties, samples with a high C/O and C/H ratio produce syngas with a high HHV. In the case of the samples with high C/O and C/H ratios, such as Melina and Teak, they showed the highest decrease on syngas HHV as 6.8 and 6.1 MJ/kmol, respectively. On the other hand, the samples that have relatively low C/O and C/H ratios have lower syngas HHV, and are relatively less influenced by pressure. In the common temperature range for gasification (800–1000 °C), according to Baratieri et al. [79], a rise in pressure causes a loss of around 10 % of the heating value of the syngas generally. Other researches have also reported that increasing the gasifier pressure lowers the heating value of syngas [34].

The birch was chosen as feedstock for the gasification process in order to get the properties of each stream at the specific condition. The mass flow rate (kg/h), temperature (°C), pressure (bar), and composition of each stream were recorded and shown in Table 4 at the steam/biochar and CO_2/biochar ratios are 1, the gasifier temperature is 800 °C, and the gasifier pressure is 1 bar.

4. Conclusion

The thermochemical performance of different biochar samples under steam and CO_2 gasification conditions was investigated using a steady-state equilibrium CFB gasifier model developed with Aspen HYSYS software. The syngas compositions were verified with experimental data published in the literature to determine the accuracy of the CFB gasifier model before proceeding with the parametric study, and the estimated gas fractions agreed well with the actual values. In addition, the CFB gasifier model created in this work performed exceptionally well in validating solid fuels with different physicochemical properties, such as biomass, coal, blends, and biochar. This finding is crucial to the uniqueness of the study because, as mentioned earlier, it is difficult to develop a gasifier model in the Aspen HYSYS process simulator, especially one that covers a wide range of solid fuels. As a result of the reliable CFB gasifier model designed in this work, many researchers could be encouraged to employ Aspen HYSYS to simulate gasification processes in the future studies. A high gasification temperature increases the HHV of the syngas (an increase of approximately 12.5 % between 600 °C and 1000 °C), while increasing the amount of H_2O and CO_2

Table 4
The properties of streams for the selected conditions.

Stream Name	Mass Flow Rate (kg/h)	Temp. (°C)	Press. (bar)	Composition (Mole Fraction)								
				H_2	CO	CO_2	CH_4	H_2O	N_2	O_2	C	Ash
Biochar	100.00	25.0	1.0	0.3299	0.0000	0.0000	0.0000	0.0000	0.0003	0.1317	0.5378	0.0004
Fuel	99.87	25.0	1.0	0.3301	0.0000	0.0000	0.0000	0.0000	0.0003	0.1317	0.5379	0.0000
Ash	0.13	25.0	1.0	0.0000	0.0000	0.0000	0.0000	0.0000	0.0000	0.0000	0.0000	1.000
Fuel-1	4.99	25.0	1.0	0.3301	0.0000	0.0000	0.0000	0.0000	0.0003	0.1317	0.5379	0.0000
Fuel-2	94.88	25.0	1.0	0.3301	0.0000	0.0000	0.0000	0.0000	0.0003	0.0000	0.5379	0.0000
Gas-1	44.99	400.0	1.0	0.0814	0.0040	0.3366	0.0496	0.5283	0.0001	0.0000	0.0000	0.0000
Liq-1	0.00	400.0	1.0	0.0814	0.0040	0.3366	0.0496	0.5283	0.0001	0.0000	0.0000	0.0000
Steam	100.00	250.0	1.0	0.0000	0.0000	0.0000	0.0000	1.0000	0.0000	0.0000	0.0000	0.0000
CO2	100.00	250.0	1.0	0.0000	0.0000	1.0000	0.0000	0.0000	0.0000	0.0000	0.0000	0.0000
Out	200.00	250.0	1.0	0.0000	0.0000	0.2904	0.0000	0.7096	0.0000	0.0000	0.0000	0.0000
Agent-1	40.00	250.0	1.0	0.0000	0.0000	0.2904	0.0000	0.7096	0.0000	0.0000	0.0000	0.0000
Agent-2	160.00	250.0	1.0	0.0000	0.0000	0.2904	0.0000	0.7096	0.0000	0.0000	0.0000	0.0000
Gas-2	43.09	400.0	1.0	0.0000	0.0000	0.3892	0.0000	0.6107	0.0001	0.0000	0.0000	0.0000
Gas-3	1.90	400.2	1.0	0.6029	0.0297	0.0000	0.3675	0.0000	0.0000	0.0000	0.0000	0.0000
Gas-4	298.00	800.0	1.0	0.347	0.2865	0.1727	0.0004	0.1932	0.0002	0.0000	0.0000	0.0000
Liq-2	0.00	800.0	1.0	0.347	0.2865	0.1727	0.0004	0.1932	0.0002	0.0000	0.0000	0.0000
Gas-5	300.00	792.8	1.0	0.351	0.2825	0.17	0.0062	0.1901	0.0002	0.0000	0.0000	0.0000
Gas-6	155.30	800.0	1.0	0.4195	0.5733	0.0000	0.007	0.0000	0.0003	0.0000	0.0000	0.0000
Gas-7	184.60	788.4	1.0	0.2695	0.0508	0.3055	0.0055	0.3417	0.0001	0.0000	0.0000	0.0000
Air	1000.00	100.0	1.0	0.0000	0.0000	0.0000	0.0000	0.0000	0.7900	0.2100	0.0000	0.0000
Gas-8	1185.00	1000.0	1.0	0.0000	0.0000	0.0738	0.0000	0.1324	0.6567	0.1368	0.0000	0.0000
Liq-3	0.00	1000.0	1.0	0.0000	0.0000	0.0738	0.0000	0.1324	0.6567	0.1368	0.0000	0.0000
Gas-9	235.10	1000.0	1.0	0.0000	0.0000	0.3574	0.0000	0.6413	0.0000	0.0000	0.0000	0.0000
Gas-10	949.40	1000.0	1.0	0.0000	0.0000	0.0000	0.0000	0.0000	0.8276	0.1724	0.0000	0.0000
Gas-11	350.40	930.1	1.0	0.1848	0.2525	0.2000	0.0031	0.3588	0.0001	0.0000	0.0000	0.0000
Syngas	251.00	700.0	1.0	0.2883	0.3939	0.3119	0.0048	0.0000	0.0000	0.0000	0.0000	0.0000
Waste	99.48	1290.0	1.0	0.0000	0.0000	0.0000	0.0000	0.9997	0.0003	0.0000	0.0000	0.0000

supplied to the reactor decreases the HHV of the syngas, as shown by parametric studies. As the steam/biochar ratio increased from 0.0 to 2.0, syngas HHV experienced an average of 33.96 % decline, while the CO_2/biochar ratio improved from 0.0 to 2.0, syngas HHV experienced an average of 21.28 % decrease. Moreover, the results showed that steam gasification of biochar samples with high carbon content produces H_2-rich syngas with high heating value. The optimum gasification temperature is 700 °C, the gasification pressure is 1 bar, and the ideal steam/biochar and CO_2/biochar ratios are between 0.2 and 0.3 and 0.5 and 1.0, depending on the biochar properties.

CRediT authorship contribution statement

Uğur Özveren: Conceptualization, Data Curation, Formal analysis, Funding acquisition, Investigation, Data curation, Methodology, Project Administration, Resources, Software, Supervision, Validation, Visualization, Writing – original draft Preparation, Writing – review & editing. **Furkan Kartal:** Investigation, Data Curation, Software, Validation, Visualization, Writing – original draft Preparation, Writing – review & editing. **Senem Sezer:** Software, Validation, Visualization, Writing – original draft Preparation, Writing – review & editing.

Declaration of Competing Interest

The authors declare that they have no known competing financial interests or personal relationships that could have appeared to influence the work reported in this paper.

References

[1] D. Zhang, J. Wang, Y. Lin, Y. Si, C. Huang, J. Yang, B. Huang, W. Li, Present situation and future prospect of renewable energy in China, Renew. Sustain. Energy Rev. 76 (2017) 865–871.

[2] J. Li, W. Cheng, Comparative life cycle energy consumption, carbon emissions and economic costs of hydrogen production from coke oven gas and coal gasification, Int. J. Hydrog. Energy 45 (51) (2020) 27979–27993.

[3] T. Pachiannan, W. Zhong, S. Rajkumar, Z. He, X. Leng, Q. Wang, A literature review of fuel effects on performance and emission characteristics of low-temperature combustion strategies, Appl. Energy 251 (2019), 113380.

[4] F. Ebrahimian, K. Karimi, Efficient biohydrogen and advanced biofuel coproduction from municipal solid waste through a clean process, Bioresour. Technol. 300 (2020), 122656.

[5] J.C. Solarte-Toro, J.A. González-Aguirre, J.A.P. Giraldo, C.A.C. Alzate, Thermochemical processing of woody biomass: a review focused on energy-driven applications and catalytic upgrading, Renew. Sustain. Energy Rev. 136 (2021), 110376.

[6] P. Mishra, G. Lakshmi, S. Mishra, D. Avasthi, H.C. Swart, A.P. Turner, Y.K. Mishra, A. Tiwari, Electrocatalytic biofuel cell based on highly efficient metal-polymer nano-architectured bioelectrodes, Nano Energy 39 (2017) 601–607.

[7] B. Nahak, S. Preetam, D. Sharma, S. Shukla, M. Syväjärvi, D.-C. Toncu, A. Tiwari, Advancements in net-zero pertinency of lignocellulosic biomass for climate neutral energy production, Renew. Sustain. Energy Rev. 161 (2022), 112393.

[8] S.A. Zaman, S. Ghosh, A generic input-output approach in developing and optimizing an Aspen Plus steam-gasification model for biomass, Bioresour. Technol. (2021), 125412.

[9] A.V. Bridgwater, Renewable fuels and chemicals by thermal processing of biomass, Chem. Eng. J. 91(2-3) (2003) 87–102.

[10] M. Puig-Gamero, J. Argudo-Santamaria, J. Valverde, P. Sánchez, L. Sanchez-Silva, Three integrated process simulation using aspen plus®: Pine gasification, syngas cleaning and methanol synthesis, Energy Convers. Manag. 177 (2018) 416–427.

[11] J.S. Tumuluru, Biomass preprocessing and pretreatments for production of biofuels: mechanical, chemical and thermal methods, CRC Press,, 2018.

[12] G. Mirmoshtaghi, H. Li, E. Thorin, E. Dahlquist, Evaluation of different biomass gasification modeling approaches for fluidized bed gasifiers, Biomass-.-. Bioenergy 91 (2016) 69–82.

[13] F. Ju, H. Chen, H. Yang, X. Wang, S. Zhang, D. Liu, Experimental study of a commercial circulated fluidized bed coal gasifier, Fuel Process. Technol. 91 (8) (2010) 818–822.

[14] N. Nipattummakul, I. Ahmed, S. Kerdsuwan, A.K. Gupta, High temperature steam gasification of wastewater sludge, Appl. Energy 87 (12) (2010) 3729–3734.

[15] G. Lopez, M. Artetxe, M. Amutio, J. Alvarez, J. Bilbao, M. Olazar, Recent advances in the gasification of waste plastics. A critical overview, Renew. Sustain. Energy Rev. 82 (2018) 576–596.

[16] E. Veca, A. Adrover, Isothermal kinetics of char-coal gasification with pure CO_2, Fuel 123 (2014) 151–157.

[17] N.A. Ahmad, K.A. Al-attab, Z.A. Zainal, P. Lahijani, Microwave assisted steam-CO_2 char gasification of oil palm shell, Bioresour. Technol. Rep. 15 (2021), 100785.

[18] M. Zhai, Y. Zhang, P. Dong, P. Liu, Characteristics of rice husk char gasification with steam, Fuel 158 (2015) 42–49.

[19] A. Anniwaer, N. Chaihad, A.C.A. Zahra, T. Yu, Y. Kasai, S. Kongparakul, C. Samart, A. Abudula, G. Guan, Steam co-gasification of Japanese cedarwood and its commercial biochar for hydrogen-rich gas production, Int. J. Hydrog. Energy (2021).

[20] S. Chaudhari, S. Bej, N. Bakhshi, A. Dalai, Steam gasification of biomass-derived char for the production of carbon monoxide-rich synthesis gas, Energy fuels 15 (3) (2001) 736–742.

[21] A. AlNouss, P. Parthasarathy, M. Shahbaz, T. Al-Ansari, H. Mackey, G. McKay, Techno-economic and sensitivity analysis of coconut coir pith-biomass gasification using ASPEN PLUS, Appl. Energy 261 (2020), 114350.
[22] D. Baruah, D. Baruah, Modeling of biomass gasification: a review, Renew. Sustain. Energy Rev. 39 (2014) 806–815.
[23] A.J. Keche, A.P.R. Gaddale, R.G. Tated, Simulation of biomass gasification in downdraft gasifier for different biomass fuels using ASPEN PLUS, Clean. Technol. Environ. Policy 17 (2) (2015) 465–473.
[24] W. Tan, Q. Zhong, Simulation of hydrogen production in biomass gasifier by ASPEN PLUS, 2010 Asia-Pacific Power and Energy Engineering Conference, IEEE, 2010, pp. 1–4.
[25] W. Doherty, A. Reynolds, D. Kennedy, Simulation of a circulating fluidised bed biomass gasifier using ASPEN Plus: a performance analysis, (2008).
[26] D.-H. Jang, H.-T. Kim, C. Lee, S.-H. Kim, Kinetic analysis of catalytic coal gasification process in fixed bed condition using Aspen Plus, Int. J. Hydrog. Energy 38 (14) (2013) 6021–6026.
[27] T.R. Paul, H. Nath, V. Chauhan, A. Sahoo, Gasification studies of high ash Indian coals using Aspen plus simulation, Mater. Today.: Proc. 46 (2021) 6149–6155.
[28] W. Duan, Q. Yu, K. Wang, Q. Qin, L. Hou, X. Yao, T. Wu, ASPEN Plus simulation of coal integrated gasification combined blast furnace slag waste heat recovery system, Energy Convers. Manag. 100 (2015) 30–36.
[29] J. Salisu, N. Gao, C. Quan, techno-economic assessment of co-gasification of rice husk and plastic waste as off-grid power source for small scale rice milling in nigeria-an aspen plus modeL, J. Anal. Appl. Pyrolysis (2021), 105157.
[30] F. Barontini, S. Frigo, R. Gabbrielli, P. Sica, Co-gasification of woody biomass with organic and waste matrices in a down-draft gasifier: An experimental and modeling approach, Energy Convers. Manag. 245 (2021), 114566.
[31] D.K. Singh, J.V. Tirkey, Modeling and multi-objective optimization of variable air gasification performance parameters using Syzygium cumini biomass by integrating ASPEN Plus with response surface methodology (RSM), Int. J. Hydrog. Energy 46 (36) (2021) 18816–18831.
[32] M. Faraji, M. Saidi, Hydrogen-rich syngas production via integrated configuration of pyrolysis and air gasification processes of various algal biomass: Process simulation and evaluation using Aspen Plus software, Int. J. Hydrog. Energy 46 (36) (2021) 18844–18856.
[33] S.G. Gopaul, A. Dutta, R. Clemmer, Chemical looping gasification for hydrogen production: a comparison of two unique processes simulated using ASPEN Plus, Int. J. Hydrog. Energy 39 (11) (2014) 5804–5817.
[34] K.K. Hoo, M.S.M. Said, Simulation of air gasification of Napier grass using Aspen plus, Sustain. Energy Technol. Assess. 50 (2022), 101837.
[35] S. Vikram, P. Rosha, S. Kumar, S. Mahajani, Thermodynamic analysis and parametric optimization of steam-CO_2 based biomass gasification system using Aspen PLUS, Energy (2021), 122854.
[36] M.W. Islam, Effect of different gasifying agents (steam, H2O2, oxygen, CO_2, and air) on gasification parameters, Int. J. Hydrog. Energy 45 (56) (2020) 31760–31774.
[37] M. Bassyouni, S.W. ul Hasan, M. Abdel-Aziz, S.-S. Abdel-hamid, S. Naveed, A. Hussain, F.N. Ani, Date palm waste gasification in downdraft gasifier and simulation using ASPEN HYSYS, Energy Conversión Manag. 88 (2014) 693–699.
[38] A.M. Gonzalez, E.E.S. Lora, J.C.E. Palacio, O.A.A. del Olmo, Hydrogen production from oil sludge gasification/biomass mixtures and potential use in hydrotreatment processes, Int. J. Hydrog. Energy 43 (16) (2018) 7808–7822.
[39] R. Milani, A. Szklo, B.S. Hoffmann, Hybridization of concentrated solar power with biomass gasification in Brazil's semiarid region, Energy Convers. Manag. 143 (2017) 522–537.
[40] F. Kartal, U. Özveren, A comparative study for biomass gasification in bubbling bed gasifier using Aspen HYSYS, Bioresour. Technol. Rep. 13 (2021), 100615.
[41] D. Pashchenko, Industrial furnaces with thermochemical waste-heat recuperation by coal gasification, Energy 221 (2021), 119864.
[42] P. Kraisornkachit, S. Vivanpatarakij, S. Amornraksa, L. Simasatitkul, S. Assabumrungrat, Performance evaluation of different combined systems of biochar gasifier, reformer and CO_2 capture unit for synthesis gas production, Int. J. Hydrog. Energy 41 (31) (2016) 13408–13418.
[43] Z. Zhang, B. Delcroix, O. Rezazgui, P. Mangin, Simulation and techno-economic assessment of bio-methanol production from pine biomass, biochar and pyrolysis oil, Sustain. Energy Technol. Assess. 44 (2021), 101002.
[44] S.A. Salaudeen, B. Acharya, A. Dutta, Steam gasification of hydrochar derived from hydrothermal carbonization of fruit wastes, Renew. Energy 171 (2021) 582–591.
[45] M. Strandberg, I. Olofsson, L. Pommer, S. Wiklund-Lindström, K. Åberg, A. Nordin, Effects of temperature and residence time on continuous torrefaction of spruce wood, Fuel Process. Technol. 134 (2015) 387–398.
[46] Q.-V. Bach, K.-Q. Tran, Ø. Skreiberg, T.T. Trinh, Effects of wet torrefaction on pyrolysis of woody biomass fuels, Energy 88 (2015) 443–456.
[47] R.H. Ibrahim, L.I. Darvell, J.M. Jones, A. Williams, Physicochemical characterisation of torrefied biomass, J. Anal. Appl. Pyrolysis 103 (2013) 21–30.
[48] L. Cao, X. Yuan, H. Li, C. Li, Z. Xiao, L. Jiang, B. Huang, Z. Xiao, X. Chen, H. Wang, Complementary effects of torrefaction and co-pelletization: Energy consumption and characteristics of pellets, Bioresour. Technol. 185 (2015) 254–262.
[49] D. Chen, K. Cen, X. Cao, J. Zhang, F. Chen, J. Zhou, Upgrading of bio-oil via solar pyrolysis of the biomass pretreated with aqueous phase bio-oil washing, solar drying, and solar torrefaction, Bioresour. Technol. 305 (2020), 123130.
[50] A. Adeleke, J. Odusote, P. Ikubanni, O. Lasode, M. Malathi, D. Paswan, The ignitability, fuel ratio and ash fusion temperatures of torrefied woody biomass, Heliyon 6 (3) (2020), e03582.
[51] M. Ahmad, H. Subawi, New Van Krevelen diagram and its correlation with the heating value of biomass, J. Agric. Environ. Manag. 2 (10) (2013) 295–301.
[52] K.A. Abdulyekeen, A.A. Umar, M.F.A. Patah, W.M.A.W. Daud, Torrefaction of biomass: production of enhanced solid biofuel from municipal solid waste and other types of biomass, Renew. Sustain. Energy Rev. 150 (2021), 111436.
[53] M. Puig-Arnavat, J.C. Bruno, A. Coronas, Review and analysis of biomass gasification models, Renew. Sustain. Energy Rev. 14 (9) (2010) 2841–2851.
[54] I.P. Silva, R.M. Lima, G.F. Silva, D.S. Ruzene, D.P. Silva, Thermodynamic equilibrium model based on stoichiometric method for biomass gasification: A review of model modifications, Renew. Sustain. Energy Rev. 114 (2019), 109305.
[55] H.M.U. Ayub, S.J. Park, M. Binns, Biomass to syngas: modified non-stoichiometric thermodynamic models for the downdraft biomass gasification, Energies 13 (21) (2020) 5668.
[56] S. Jarungthammachote, A. Dutta, Thermodynamic equilibrium model and second law analysis of a downdraft waste gasifier, Energy 32 (9) (2007) 1660–1669.
[57] J. Li, K. Xu, X. Yao, S. Chen, Prediction and optimization of syngas production from steam gasification: Numerical study of operating conditions and biomass composition, Energy Convers. Manag. 236 (2021), 114077.
[58] A. Technology, Getting Started Modeling Processes with Solids, Version l 0.2, Aspen Technology Inc.,, Cambridge, USA, 2000.
[59] M. Puig-Gamero, D. Pio, L. Tarelho, P. Sánchez, L. Sanchez-Silva, Simulation of biomass gasification in bubbling fluidized bed reactor using aspen plus®, Energy Convers. Manag. 235 (2021), 113981.
[60] M. Niu, J. Xie, S. Liang, L. Liu, L. Wang, Y. Peng, Simulation of a new biomass integrated gasification combined cycle (BIGCC) power generation system using Aspen Plus: Performance analysis and energetic assessment, Int. J. Hydrog. Energy (2021).
[61] P. Garcıa-Ibanez, A. Cabanillas, J. Sánchez, Gasification of leached orujillo (olive oil waste) in a pilot plant circulating fluidised bed reactor. Preliminary results, Biomass Bioenergy 27 (2) (2004) 183–194.
[62] C. Berrueco, J. Recari, B.M. Güell, G. Del, Alamo, Pressurized gasification of torrefied woody biomass in a lab scale fluidized bed, Energy 70 (2014) 68–78.
[63] F. Duan, B. Jin, Y. Huang, B. Li, Y. Wu, M. Zhang, Results of bituminous coal gasification upon exposure to a pressurized pilot-plant circulating fluidized-bed (CFB) reactor, Energy Fuels 24 (5) (2010) 3150–3158.
[64] J. Li, F. Li, W. Liu, Z. Liu, H. Zhan, Y. Zhang, Z. Hao, Z. Cheng, J. Huang, Y. Fang, Influence of pressure on fluidized bed gasifier: specific coal throughput and particle behavior, Fuel 220 (2018) 80–88.
[65] J. Han, Y. Liang, J. Hu, L. Qin, J. Street, Y. Lu, F. Yu, Modeling downdraft biomass gasification process by restricting chemical reaction equilibrium with Aspen Plus, Energy Convers. Manag. 153 (2017) 641–648.
[66] R. Tavares, E. Monteiro, F. Tabet, A. Rouboa, Numerical investigation of optimum operating conditions for syngas and hydrogen production from biomass gasification using Aspen Plus, Renew. Energy 146 (2020) 1309–1314.
[67] A.A. Ahmad, N.A. Zawawi, F.H. Kasim, A. Inayat, A. Khasri, Assessing the gasification performance of biomass: a review on biomass gasification process conditions, optimization and economic evaluation, Renew. Sustain. Energy Rev. 53 (2016) 1333–1347.
[68] S. Heyne, M. Seemann, T.J. Schildhauer, Coal and Biomass Gasification for SNG Production, Synthetic Natural Gas from Coal and Dry Biomass, and Power-to-Gas Applications (2016) 5–40.
[69] N. Ramzan, A. Ashraf, S. Naveed, A. Malik, Simulation of hybrid biomass gasification using Aspen plus: a comparative performance analysis for food, municipal solid and poultry waste, Biomass-.-. bioenergy 35 (9) (2011) 3962–3969.
[70] L.T.C. Montoya, S. Lain, M. Issa, A. Ilinca, Renewable Energy Systems, Hybrid Renewable Energy Systems and Microgrids, Elsevier, 2021, pp. 103–177.
[71] Y. Cao, Y. Bai, J. Du, Air-steam gasification of biomass based on a multi-composition multi-step kinetic model: a clean strategy for hydrogen-enriched syngas production, Sci. Total Environ. 753 (2021), 141690.
[72] Y. Zhang, C. Ke, Y. Gao, S. Liu, Y. Pan, N. Zhou, Y. Wang, L. Fan, P. Peng, B. Li, Syngas production from microwave-assisted air gasification of biomass: Part 2 model validation, Renew. Energy 140 (2019) 625–632.
[73] M. Hussain, L.D. Tufa, R.N.A.B.R. Azlan, S. Yusup, H. Zabiri, Steady state simulation studies of gasification system using palm kernel shell, Procedia Eng. 148 (2016) 1015–1021.
[74] E. Monteiro, T.M. Ismail, A. Ramos, M. Abd El-Salam, P. Brito, A. Rouboa, Assessment of the miscanthus gasification in a semi-industrial gasifier using a CFD model, Appl. Therm. Eng. 123 (2017) 448–457.
[75] S. Sezer, F. Kartal, U. Özveren, Prediction of chemical exergy of syngas from downdraft gasifier by means of machine learning, Therm. Sci. Eng. Prog. (2021), 101031.
[76] A.K. Sharma, Equilibrium modeling of global reduction reactions for a downdraft (biomass) gasifier, Energy Convers. Manag. 49 (4) (2008) 832–842.
[77] M.R. Mahishi, D. Goswami, Thermodynamic optimization of biomass gasifier for hydrogen production, Int. J. Hydrog. Energy 32 (16) (2007) 3831–3840.
[78] M. Wiatowski, K. Kapusta, M. Ludwik-Pardała, K. Stańczyk, Ex-situ experimental simulation of hard coal underground gasification at elevated pressure, Fuel 184 (2016) 401–408.
[79] M. Baratieri, P. Baggio, L. Fiori, M. Grigiante, Biomass as an energy source: thermodynamic constraints on the performance of the conversion process, Bioresour. Technol. 99 (15) (2008) 7063–7073.